The squeezes, stretches, and whirls of turbulence

Perry L. Johnson

Citation: Physics Today **74**, 4, 46 (2021); doi: 10.1063/PT.3.4725
View online: https://doi.org/10.1063/PT.3.4725
View Table of Contents: https://physicstoday.scitation.org/toc/pto/74/4
Published by the American Institute of Physics

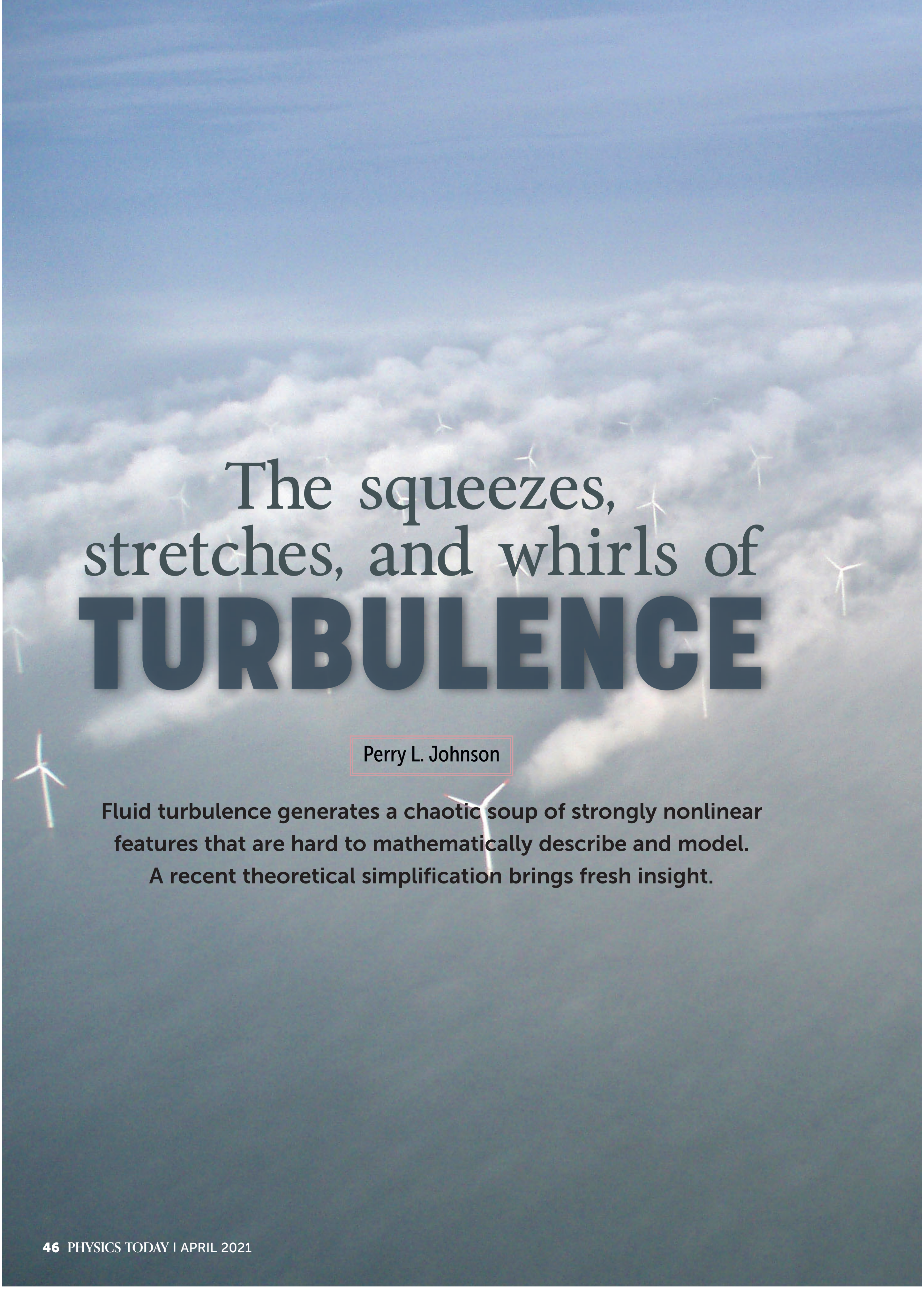

The squeezes, stretches, and whirls of TURBULENCE

Perry L. Johnson

Fluid turbulence generates a chaotic soup of strongly nonlinear features that are hard to mathematically describe and model. A recent theoretical simplification brings fresh insight.

Perry Johnson is an assistant professor of mechanical and aerospace engineering at the University of California, Irvine.

In his famous *Lectures on Physics*, Richard Feynman reflected on a "physical problem that is common to many fields, that is very old, and that has not been solved. It is not the problem of finding new fundamental particles, but something left over from a long time ago—over a hundred years. . . . It is the analysis of *circulating or turbulent fluids*."[1] Even today in the age of supercomputers, the need for understanding, modeling, and predicting aspects of turbulent flows has, if anything, increased. Reliably simulating turbulent flows still requires more theoretical advances, and Feynman's vision of "solving the problem of turbulence" remains elusive.

Turbulent flows are characterized by apparently random, chaotic motions. And they are everywhere: They govern the efficiency of gas turbine engines, the workhorses of modern power generation and aerospace propulsion, and of large-scale wind farms, a key technology for renewable energy (see the article by John Dabiri, PHYSICS TODAY, October 2014, page 66). In the past year, turbulent flows produced by coughs and sneezes, as shown in figure 1a, have come to the forefront because of the COVID-19 pandemic.[2] What's more, turbulence physics is vital for estimating and mitigating the impact of deep-sea oil spills, informing parameterizations for weather prediction and global climate models, and quantifying the turbulence-induced damage on red blood cells in artificial heart valves and blood pumps. Turbulence is at work even in our leisure; it alters the aerodynamic behavior of, for example, race cars, golf balls, baseballs, and soccer balls—as illustrated by the irregular motion of the controversial Jabulani soccer balls specially designed for the 2010 World Cup. (For more on soccer-ball dynamics, see the article by John Eric Goff, PHYSICS TODAY, July 2010, page 62.)

For many turbulent scenarios, analytical solutions to the equations of motion aren't possible, and the computational cost of simulations is unwieldy. For example, in large arrays of wind turbines, such as the ones shown here, a turbulent wake of lower-speed air forms behind each turbine and diminishes the power output of downwind ones caught in the wake.[3] The smallest turbulent motions in that flow are less than a millimeter, whereas

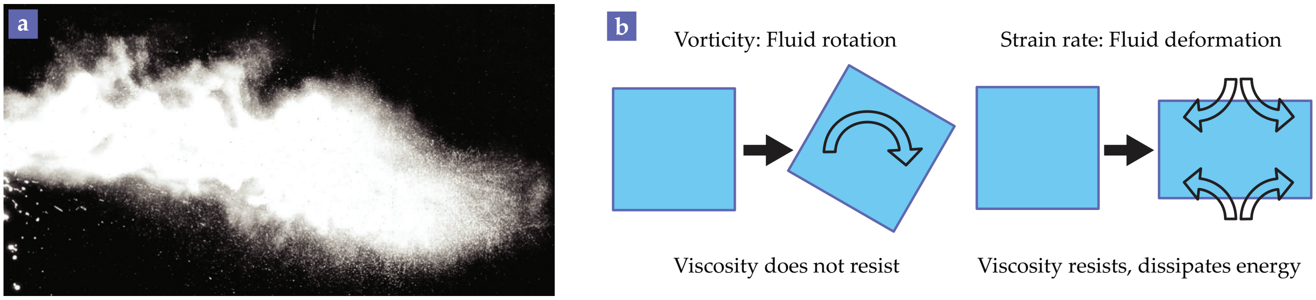

FIGURE 1. TURBULENT FLOWS, which occur in various systems, share two forms of motion. From the wind turbines seen in the opening image to **(a)** the sneeze droplets pictured here (reproduced from ref. 2), turbulence contains strong coherent regions where **(b)** fluid (blue square) is subjected to rotations, which are quantified by the vorticity, or to deformations, which are quantified by the strain rate. Viscosity does not resist rotations, but it does resist deformations. As a result, the strain rate results in energy dissipation.

the farm extends for kilometers. A brute-force simulation with millimeter resolution over a kilometer range is not currently possible, nor will it be in the foreseeable future. A similar combination of small and large scales holds true for many important turbulent flows, such as the aerodynamic flow over a car or airplane[4] and the complex flow through airplane engines.

Despite emerging in such disparate physical systems, turbulent flows tend to display remarkably similar characteristics—although different types of turbulent flows have enough unique qualities and behaviors to warrant discipline-specific specialized research. However, the emergence of universal attributes motivates cross-disciplinary effort to analyze and compute turbulence. One such attribute is the enhancement of energy dissipation through the production of motion on a progressively smaller scale. Understanding the physical mechanisms behind that dissipation is vital for constructing accurate theories and computational models of turbulence.

Energy cascade

A detailed description of a turbulent flow involves a three-dimensional field of velocity vectors **u**, which vary erratically in space and time. Turbulent velocity fluctuations are not completely unorganized in space and time; on closer inspection, they have a degree of coherence not on a set of discrete length scales or frequencies but in an intrinsically broadband manner. The faster or larger the overall flow or the lower the fluid viscosity, the wider the range of length scales and frequencies dynamically active in a turbulent flow. The low viscosities of common fluids such as air and water ($\nu_{\text{air}} = 10^{-5}$ m^2/s and $\nu_{\text{water}} = 10^{-6}$ m^2/s) explain why turbulent flows with a wide range of scales are encountered frequently in science and engineering.

The multiscale nature of turbulence can be thought of as a superposition of motions with spatial coherence of a given length scale. The wide range of scales in a turbulent flow results from one of the most fundamental and universal aspects of turbulence: the energy cascade. It is the process by which kinetic energy generated at large scales is passed successively from smaller scale to smaller scale until the motions are so small that viscosity prevents the formation of even smaller motions because it dissipates the energy into heat. The process occurs rapidly and enhances the overall rate of energy dissipation far above that of smooth laminar flows.

The energy cascade is an important consideration for computer simulations in scientific discovery and engineering design. For the wind-farm example discussed earlier, any attempt at simulation must use coarser-grain resolution than a millimeter and thus end up severely underresolved. To compensate for that lack of resolution, kinetic energy is artificially removed from simulations to mimic the cascade of energy from resolved scales to unresolved

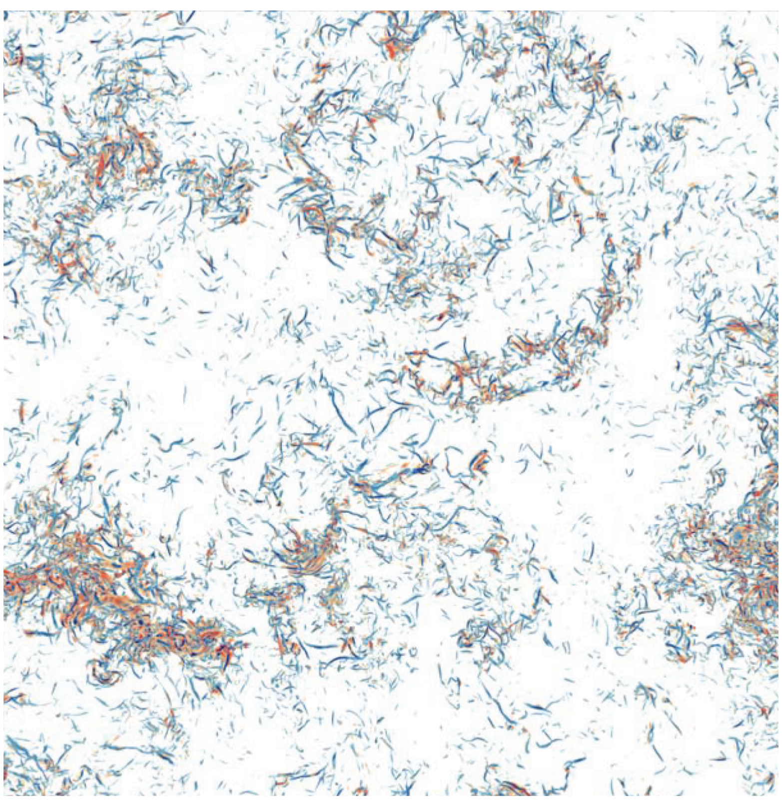

FIGURE 2. STRETCHING AND ROTATING regions. In this turbulence visualization, most of the fluid has low activity, but certain regions are characterized by large-magnitude vorticity (blue) and large-magnitude strain rate (red). (From ref. 6.)

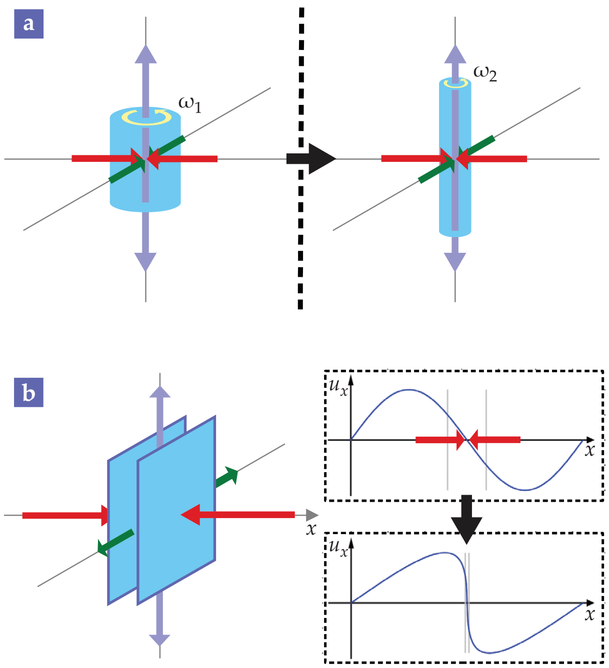

FIGURE 3. ENERGY DISSIPATES at an enhanced rate from a combination of two mechanisms. **(a)** When under strain (red, green, and violet arrows), a fluid vortex rotating at a rate ω_1 gets stretched out, and the result is a higher rotation rate ω_2. Energy passes to successively smaller and smaller vortices, a phenomenon known as vortex stretching. **(b)** Regions of strong strain rate can also self-amplify. In that mechanism, a sheet-like region of high compression naturally tends to grow thinner as the strain rate gets steeper because faster-moving fluid (peaks in graphs of u_x as a function of position x) overtakes slower fluid ahead of it and squeezes the fluid particle.

ones. Doing so accurately requires understanding the mechanisms behind the energy cascade.

Stretches and whirls

In a 1922 rhyming verse, British meteorologist Lewis Richardson was the first to describe the energy cascade in turbulent flows: "Big whirls have little whirls that feed on their velocity, and little whirls have lesser whirls and so on to viscosity."[5] The dynamics of "whirls" or eddies—that is, localized rotations in a flow—has since proven key to the phenomenology of the energy cascade.

In the continuum approximation of fluid dynamics, a fluid particle is defined as an effectively infinitesimal volume of fluid at a specific location. In addition to the particle's velocity, its dynamics is described by two quantities: the vorticity and the strain rate. The vorticity gives the rate at which a fluid particle at a given position is rotating. The strain-rate tensor describes the local rate at which a fluid particle is getting stretched and squeezed. In figure 1b, for example, strain deforms an initially square fluid particle into a rectangle. Pressure forces keep a fluid particle's volume constant in flows with velocities well below the speed of sound, so a particle that is stretched in one direction will necessarily be squeezed in another.

Mathematically, the vorticity and the strain rate involve the gradient of the velocity vector, $\nabla\mathbf{u}$, a 3×3 rank-2 tensor that describes the local variation of the three components of velocity in each of the three coordinate directions. The strain rate $\mathbf{S}$ is defined as $\mathbf{S} = \frac{1}{2}[\nabla\mathbf{u} + (\nabla\mathbf{u})^{\mathrm{T}}]$, in terms of the gradient tensor and its transpose, and the vorticity vector $\boldsymbol{\omega}$ is defined as $\boldsymbol{\omega} = \nabla \times \mathbf{u}$. The magnitude squared of the velocity gradient tensor, measured using the square root of the sum of the absolute squares of the tensor elements, is the sum of the strain-rate and vorticity magnitudes, $\|\nabla\mathbf{u}\|^2 = \|\mathbf{S}\|^2 + \frac{1}{2}|\boldsymbol{\omega}|^2$.

But those two components are physically distinct, as highlighted by their relationship to viscosity. A fluid's viscosity ν quantifies how much the fluid resists deformation by the strain rate. That resistance dissipates kinetic energy into heat at a rate $\epsilon = 2\nu\|\mathbf{S}\|^2$. Viscous forces do not resist rotation, so vorticity incurs no similar energy dissipation.

Figure 2 shows regions with large-magnitude vorticity and strain rate in a simulation of a stirred fluid in a periodic box.[6] The soup of turbulence contains mostly regions with low activity intermittently dispersed with coherent regions of high vorticity and high strain rate.

Vortex stretching

In the years after the publication of Richardson's verse, the dynamics of vorticity has commonly been associated with the energy cascade, even though vorticity doesn't directly cause energy dissipation. A phenomenon known as vortex stretching is widely used to explain the connection. When a vortex—a compact tube-like region of vorticity—is pulled by the fluid's straining motion along the axis of rotation, as depicted in figure 3a, the cross section of the vortex shrinks. Conservation of angular momentum dictates that the rotation rate must increase, similar to when spinning figure skaters pull in their arms to rotate faster. The result is a larger-magnitude vorticity in a smaller vortex. The region of coherent strain rate typically spans a slightly larger scale than the vortex and, through the work involved in stretching the vortex, passes energy from larger to smaller scales.

The historical explanation for the energy cascade was successive vortex-stretching events,[7] an idea introduced in a 1938 paper by G. I. Taylor. After careful measurements of a model turbulent air system—produced by placing a square grid of cylindrical bars in a wind tunnel—he wrote, "It seems that the stretching of vortex filaments must be regarded as the principal mechanical cause of the high rate of dissipation which is associated with turbulent motion."[8] A decade later Lars Onsager echoed that assessment in his theoretical treatment of turbulence: "Since the circulation of a vortex tube is conserved, the vorticity will increase whenever a vortex tube is stretched. . . . This process tends to make the texture of the motion ever finer, and greatly accelerates the viscous dissipation."[9] Despite the prevailing belief that the energy cascade is driven by vortex stretching, a precise connection between the two has remained elusive until recently, as will be discussed below.

Work in the past few decades has suggested an alternative mechanism called strain self-amplification to explain how energy passes from larger to smaller motions.[10] In strain self-amplification, shown schematically in figure 3b, a strong compressive strain rate naturally steepens as faster-moving fluid (peaks in the graphs of velocity) overtakes slower-moving fluid in its path. The effect is analogous to an ocean wave steepening before it breaks. Physically, strain self-amplification reduces the size of the region being squeezed and distributes the associated

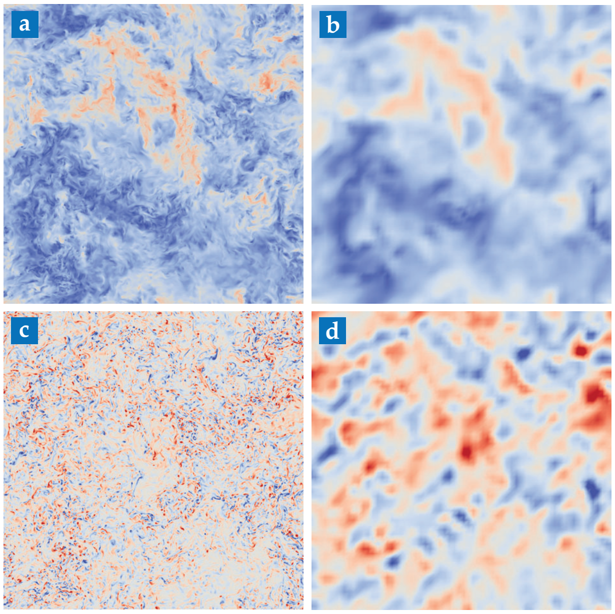

FIGURE 4. A STIRRED FLUID simulated in a periodic box displays turbulence in its three-dimensional flow. **(a)** A 2D slice showing the magnitude of the flow's velocity (red, high velocity; blue, low velocity) includes coherent motions of various sizes, including very small-scale features. **(b)** A technique called spatial filtering makes the simulation easier by sacrificing the resolution of small-scale motions. **(c)** The velocity gradient, typified by the vorticity seen here, reveals the smallest-scale motions in turbulence. **(d)** Spatially filtered vorticity, and by extension filtered velocity gradients, highlight motions at a chosen length scale. Filtered velocity gradients thus provide a basis for quantifying how energy passes between different scales.

kinetic energy toward smaller scales of motion. Similar to vortex stretching, successive self-amplification events can explain the energy cascade.

Navier–Stokes equation

To move from simplified descriptions of vortex stretching and strain self-amplification to the chaotic reality of turbulent flow requires a quantitative description. The Navier–Stokes equation encapsulates the law of momentum conservation for a fluid flow. In the simplest form, it can be written as a partial differential equation of the velocity vector field:

$$\frac{\partial \mathbf{u}}{\partial t} + \mathbf{u} \cdot \nabla \mathbf{u} = -\frac{1}{\rho} \nabla p + \nu \, \nabla^2 \mathbf{u} \,.$$

On the right side of the equation, forces due to pressure gradients ∇p and viscosity ν accelerate a fluid of mass density ρ.

Acoustic waves and electromagnetic radiation propagate at speeds set by either the medium or physical constants, such as the vacuum permittivity. As a result, excitation at a single frequency typically results in a single-frequency field. The momentum of a fluid particle, on the other hand, propagates at the local fluid velocity, which in turn is proportional to the momentum. That property generates the nonlinear term in the Navier–Stokes equation $\mathbf{u} \cdot \nabla \mathbf{u}$, which leads to vortex stretching and strain self-amplification.

Analytical solutions aren't possible in the Navier–Stokes equation for turbulent flows. But insights into the flow's nonlinear dynamics are possible if the equation is reframed in terms of the velocity gradient field $\nabla \mathbf{u}$ instead of the velocity field $\mathbf{u}$ and if the fluid particles are treated as independent of the influence of neighboring particles. Although that autonomous-particle assumption is a severe simplification, it enables exact analytical solutions. The result, called the restricted Euler equation, is drastically simplified with only a few degrees of freedom.

In 1982 Patrick Vieillefosse demonstrated that for all initial conditions, the restricted Euler equation leads to a singularity in finite time—that is, the velocity gradient magnitude $\|\nabla \mathbf{u}\|$ becomes infinite at some specific time.[11] The underlying cause of that singularity is clear from the equation for the growth in velocity gradient magnitude,

$$\frac{d}{dt}\left(\frac{1}{2}\|\nabla \mathbf{u}\|^2\right) = \underbrace{-\mathrm{Tr}\,(\mathbf{S} \cdot \mathbf{S} \cdot \mathbf{S})}_{P_S} + \underbrace{\frac{1}{4}\,\omega^T \cdot \mathbf{S} \cdot \omega}_{P_\omega} \,.$$

The velocity gradient's growth is driven by strain self-amplification, which happens at the rate P_S, and vortex stretching, which happens at the rate P_ω. When unopposed by the pressure and viscous forces of neighboring fluid particles, those two processes, which represent the autonomous dynamics of individual fluid particles, produce the singularity in the restricted Euler equation. Physically, the pressure and viscous forces of the Navier–Stokes equation restrain the autonomous dynamics and avert such singularities.

But along the path to the singularity, restricted Euler solutions display many traits that are observed in turbulent flow experiments and computer simulations of the full Navier–Stokes equations.[12] Those features account for why P_S and P_ω are positive on average for full Navier–Stokes solutions. In fact, only specially constructed configurations of the interactions with neighboring fluid particles can prevent nonlinear effects from establishing the statistical bias toward positive P_S and P_ω and the affiliated growth of the velocity gradient.[13]

Spatial filtering

A route to make the simulation of turbulence computationally tractable is a simplification known as spatial filtering, which is akin to changing the resolution of an image. A low-pass spatial filter operation is a weighted average over a subregion with characteristic size ℓ. Applying the filter to a 3D turbulent velocity field removes motions smaller than ℓ—for example, the velocity field in figure 4a becomes the image in figure 4b after spatial filtering.

The Navier–Stokes equation can be filtered to obtain a dynamical equation for the smoothed field shown in figure 4b. In the filtered Navier–Stokes equation, kinetic energy dissipates either through viscosity directly acting on the large-scale motions and thus dissipating energy into heat, as it does in an unfiltered field, or through energy passing to small-scale motions not represented in the filtered field. At sufficiently large filter sizes, energy removal results primarily from the latter. The field Π quantifies the rate at which that energy transfer happens.[14]

The gradient of the velocity field highlights the smallest-scale activity in a turbulent flow, as shown by the detailed features in figure 4c. That small-scale activity—namely, the vorticity and strain rate—predominantly organizes into small

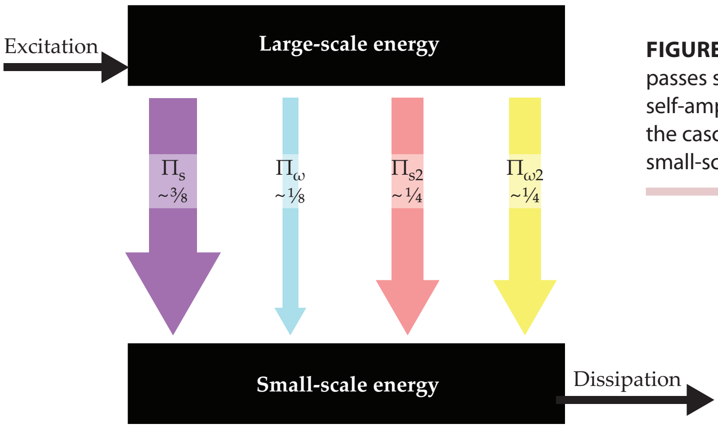

FIGURE 5. KINETIC ENERGY introduced at large scales in turbulent flows passes successively through intermediate scales at different rates due to strain self-amplification (Π_S and Π_{S2}) and vortex stretching (Π_ω and $\Pi_{\omega 2}$). At the end of the cascade, energy dissipates as heat because of viscosity's resistance to small-scale motion.

coherent regions, which resemble a chaotic soup of miniature tornadoes that swirl and stretch the participating fluid particles. The gradient of the filtered velocity field, however, accentuates organized motions of size ℓ, whatever filter size is chosen, as illustrated in figure 4d. Filtered velocity gradients thus provide a convenient definition for the scales of motion in turbulence.

A quantitative description of how turbulent motions at scale ℓ drive the cascade of energy from scales larger than ℓ to those smaller than ℓ becomes possible only if Π can be related to P_S, P_ω, and similar terms—that is, the mechanism behind turbulence cascade becomes clear if the local cascade rate can be written in terms of filtered vorticity and strain rate. Whereas previous work demonstrated a connection only in terms of truncating an infinite series, with no clear explanation as to the role of truncated terms, recent work has provided an exact relation.[15]

Cascade rate

The energy cascade rate can be written as a sum of five contributions: $\Pi = \Pi_S + \Pi_\omega + \Pi_{S2} + \Pi_{\omega 2} + \Pi_{c2}$. The first two parts, $\Pi_S = \tfrac{1}{2}\ell^2 P_S$ and $\Pi_\omega = \tfrac{1}{2}\ell^2 P_\omega$, are proportional to the strain self-amplification and vortex stretching at scale ℓ. The filtered velocity gradients tend to strongly self-amplify, just as in the restricted Euler equations, due to biases toward $P_S > 0$ and $P_\omega > 0$. Robert Betchov derived an exact relation for velocity gradients[16] that when rephrased for filtered fields states that the average contribution of Π_S to the energy cascade is three times that of Π_ω. The first two rate terms, Π_S and Π_ω, were independently identified by Maurizio Carbone and Andrew Bragg using a truncated series.[17] But solidifying a set of cascade mechanisms relied on the identification of the remaining three terms.

The next two contributions to the energy cascade, Π_{S2} and $\Pi_{\omega 2}$, have interpretations analogous to the first two terms. They arise from the amplification of smaller-scale strain rate by larger-scale strain rate and the stretching of smaller-scale vorticity by larger-scale strain rate, respectively. The final term, Π_{c2}, results from the distortion of small-scale strain–vorticity covariance by larger-scale strain rate. Whereas the first two terms represent the contribution of velocity gradient dynamics at one scale, the final three terms describe multiscale interactions. Numerical simulations have revealed that the final term contributes little, so the energy cascade rate is in practice a sum of the first four terms. Those terms precisely quantify strain self-amplification and vortex stretching along with their respective multiscale generalizations.

Figure 5 shows the fractional contribution of each term as numerically computed from turbulent solutions to the Navier–Stokes equation for a stirred fluid in a periodic box. Contrary to the theories of Taylor[8] and Onsager,[9] strain self-amplification is a bigger contribution to the energy cascade than vortex stretching, and previously unidentified multiscale interactions are a vital part of the picture. The results provide invaluable insights for improving approximation methods for computing an artificially smoothed version of turbulent flows, such as the coarse-grained simulation of a wind farm described earlier. Those methods depend on models that accurately represent the energy cascade to know how energy must be removed from the simulation in a point-wise manner. And a precise understanding of multiscale strain self-amplification and vortex stretching can lead directly to more accurate models.[15]

Vortex stretching and strain self-amplification are universal aspects of turbulent flows, so results in simple flows should illuminate modeling efforts for a wide range of complex flows, including wind farms, gas turbine engines, and aerodynamic vehicles. For the time being, experimental measurements of both scaled-down replicas and expensive full-scale systems remain indispensable to scientific discovery and engineering design. But developments in turbulence theory and modeling will help propel computer simulation into a more central role in design and analysis. Many applications will require extending the current models to include additional physical phenomena such as heat and mass transport in combustion engines, flows with density stratification in oceans, compressible flows for high-speed flight, flows in a magnetic field in astrophysics, and flows with small particles and drops.

REFERENCES

1. R. P. Feynman, R. P. Leighton, M. Sands, *The Feynman Lectures on Physics*, vol. 1, Addison–Wesley (1964), sec. 3-7.
2. L. Bourouiba, *JAMA* **323**, 1837 (2020).
3. R. J. A. M. Stevens, C. Meneveau, *Annu. Rev. Fluid Mech.* **49**, 311 (2017).
4. P. R. Spalart, *Int. J. Heat Fluid Flow* **21**, 252 (2000).
5. L. F. Richardson, *Weather Prediction by Numerical Process*, Cambridge U. Press (1922), p. 66.
6. D. G. Vlaykov, M. Wilczek, *J. Fluid Mech.* **861**, 422 (2019).
7. H. Tennekes, J. L. Lumley, *A First Course in Turbulence*, MIT Press (1972).
8. G. I. Taylor, *Proc. R. Soc. London A*, **164**, 15 (1938), p. 23.
9. L. Onsager, *Nuovo Cimento* **6**, 279 (1949), p. 282.
10. A. Tsinober, *An Informal Conceptual Introduction to Turbulence*, 2nd ed., Springer (2009).
11. P. Vieillefosse, *J. Phys. (France)* **43**, 837 (1982).
12. C. Meneveau, *Annu. Rev. Fluid Mech.* **43**, 219 (2011).
13. A. Vela-Martín, J. Jiménez, *J. Fluid Mech.* **915**, A36 (2021).
14. M. Germano, *J. Fluid Mech.* **238**, 325 (1992).
15. P. L. Johnson, *Phys. Rev. Lett.* **124**, 104501 (2020).
16. R. Betchov, *J. Fluid Mech.* **1**, 497 (1956).
17. M. Carbone, A. D. Bragg, *J. Fluid Mech.* **883**, R2 (2020).

PT